

General Disclaimer

One or more of the Following Statements may affect this Document

- This document has been reproduced from the best copy furnished by the organizational source. It is being released in the interest of making available as much information as possible.
- This document may contain data, which exceeds the sheet parameters. It was furnished in this condition by the organizational source and is the best copy available.
- This document may contain tone-on-tone or color graphs, charts and/or pictures, which have been reproduced in black and white.
- This document is paginated as submitted by the original source.
- Portions of this document are not fully legible due to the historical nature of some of the material. However, it is the best reproduction available from the original submission.

NAS 5-5603

+

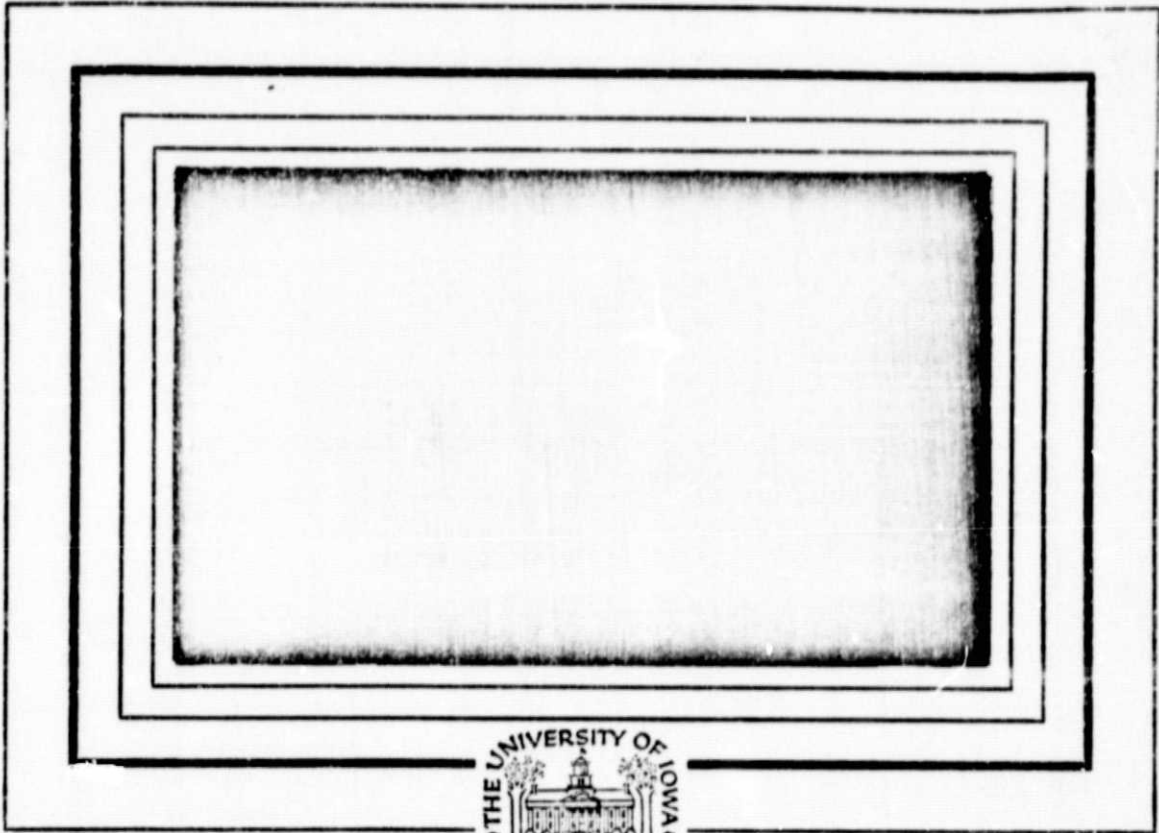
NAS 2-6563

N75-24605

Unclass
21430

G3/90

(NASA-CR-142761) PLASMA IN THE JOVIAN
MAGNETOSPHERE (Iowa Univ.) 48 p HC \$3.75
CSCL 03B



Department of Physics and Astronomy
THE UNIVERSITY OF IOWA

Iowa City, Iowa 52242

PLASMA IN THE JOVIAN MAGNETOSPHERE

by

C. K. Goertz

Department of Physics and Astronomy
University of Iowa
Iowa City, Iowa 52242

April 1975

ABSTRACT

It is shown that the plasma in Jupiter's ionosphere is collisionless above a certain level. In the outer magnetosphere where the rotational force dominates the gravitational force the collisionless plasma has a beam like distribution and gives rise to a two stream instability. This leads to trapping of plasma in the centrifugally dominated region of the magnetosphere. Plasma is lost via recombination. Equilibrium trapped particle densities are calculated by requiring a balance between trapping by wave-particle interaction and loss by recombination. The results are compared with recent observations from Pioneer 10. We indicate that the observations require an unexplained ion-heating mechanism. Some consequences of the model are discussed.

1. INTRODUCTION

A knowledge of the distribution of low energy plasma in the Jovian magnetosphere is of fundamental importance for our understanding of the magnetic field structure and hence energetic particle measurements made by Pioneer 10 and 11. In particular, Smith et al. [1974] have shown that beyond $10 R_J$ the magnetic field differs markedly from that of a (tilted and displaced) dipole. They infer from their measurements the existence of a current sheet which requires the existence of considerable plasma densities. Frank et al. [1975] have reported measurements of low energy ($E \sim 100 - 400$ eV) protons which indicate relatively large densities of plasma between $3 R_J$ and $15 R_J$. In section 2 we will review some of the published models for the distribution of low energy plasma in the Jovian magnetosphere. We will point out that none of these are completely consistent with the results of Frank et al. Frank et al. observe protons with large pitch angles which must be trapped in the outer magnetosphere. Thus the model of e.g. Melrose [1967] which does not include trapped particles, is inconsistent with observations. Other authors have claimed that Coulomb scattering of photoelectrons, released from the Jovian ionosphere, will provide a sufficiently strong trapping mechanism. We believe, however, that this mechanism requires unreasonably high densities to be effective. And furthermore we will show in section 2 that the distribution function in the magnetosphere

of the particles released from the ionosphere is beam like and unstable against a Landau resonant mode. Wave particle interaction due to this instability is a much more effective trapping mechanism than ordinary Coulomb collisions.

Using quasi-linear theory we calculate the diffusion in velocity space arising from this instability. We will argue that the conditions of strong diffusion prevail in the Jovian magnetosphere. We then determine the total density in the Jovian magnetosphere by requiring that the loss of trapped particles (due to recombination) is balanced by the diffusion in velocity space. This is done in section 3.

The resulting distribution function of trapped particles has a small perpendicular temperature but a rather large parallel temperature, where perpendicular and parallel refer to directions relative to the magnetic field. This is clearly at variance with the results of Frank et al. who report rather large perpendicular temperatures (no measurement of parallel temperatures is available as yet). In section 4 we suggest two possible reasons for this. The trapped particles will, of course, undergo collisions which will tend to reduce the temperature anisotropy. The time scale for collisions is several hours and this process may be effective. Another suggestion follows the work by Kern [1962] who has shown that a sudden compression of the earth magnetosphere by the solar wind and the subsequent propagation of a compression pulse through the magnetosphere can lead to a large

increase of perpendicular energy. It is well known by now that the Jovian magnetosphere is extremely variable in size and it may be thought that the intermittent compressions of the Jovian magnetosphere result in an enhanced perpendicular energy density of the protons. This process is investigated in section 4. Unfortunately both processes cannot account for the large energies observed inside the orbit of the moon Io. Finally, a brief discussion of some of the consequences of the proposed model plasma distribution will conclude the paper. To simplify the treatment we will neglect the tilt of the magnetic dipole with respect to the rotational axis and treat only the case of the dipole axis being aligned with the rotational axis.

2. DISTRIBUTION FUNCTIONS IN THE MAGNETOSPHERE

In a frame which corotates with the planet particles experience a gravitational and centrifugal force. These forces may be derived from a potential ϕ_G (geopotential) which can be written as

$$\phi_G = GM_J \left(\frac{1}{R_C} - \frac{1}{r} \right) - \Omega_J^2 r^2 \frac{\cos^2 \lambda}{2}, \quad (1)$$

where $GM_J = 1.267 \times 10^{23} \text{ cm}^3/\text{s}^2$ [Anderson et al. 1974]

$$R_C = 0.958 R_J = 67,907 \text{ km} \quad [\text{Michel and Sturrock 1974}]$$

$$\Omega_J = 1.76 \times 10^{-4} \text{ s}^{-1}$$

[see e.g. Gledhill 1967, Piddington 1967, Melrose 1967, Ioannidis and Brice, 1971, Michel and Sturrock 1974].

If the plasma were in statistical equilibrium everywhere inside Jupiter's magnetosphere the density would be distributed as

$$n = n_0 \exp(-m\phi_G/2KT) \quad (2)$$

where $m = m_i + m_e$

$$T = \frac{T_e + T_i}{2}$$

are the average mass and temperature of the plasma.

It was pointed out by many authors that this equation predicts an increasing plasma density in the equatorial plane ($\lambda = 0^\circ$) beyond $r = 2.3 R_J$ and it was concluded by everyone that such a distribution is unphysical. One must look for some physical constraints which limit the density in such a way that it decreases with distance in some regular manner.

One group of authors [Gledhill, Piddington, Michel and Sturrock] limit the plasma density by requiring that the corotational energy density ($\frac{1}{2} N m \Omega^2 r^2$) not exceed the magnetic field energy density ($B^2/8\pi$). For a magnetic dipole field this leads to a $1/r^8$ decrease of the plasma density. The critical density in this model even at $r = 10 R_J$ is larger than 10^4 cm^{-3} . It is questionable whether the density ever reaches such a value at $10 R_J$. If the density were as high as this one should have observed considerable distortions of the magnetic field inside $10 R_J$. This was, however, not the case [Smith et al. 1974]. At larger distances the field is not a dipole field any more [Smith et al. 1974] and without further knowledge of the magnetic field structure the above criterion cannot be used to predict the plasma density.

Other authors [Melrose, Ioannidis and Brice] drop the assumption of statistical equilibrium. And, indeed, Michel and Sturrock point out that the mean free path for collisions may be larger than the scale height even in the dense parts of the ionosphere. Thus we are forced to deal with a collisionless plasma and calculate the density variation from Liouville's equation. In particular the Jovian ionosphere will be essentially collisionless above a level h_S where the density has decreased to a critical value N_S so that the mean free path λ is larger than the scale height H . For a hydrogen plasma this yields:

$$\lambda_{H^+H^+} = \frac{11.4 T^{3/2}}{N_S \ln \Lambda} \left(\frac{kT}{m_i} \right)^{1/2} > H = \frac{kT}{m \phi_G(h_S)} h_S \quad (3)$$

This reduces to

$$N_S < 1.5 T \quad , \quad (4)$$

if T is measured in [$^{\circ}$ K].

The height h_S above the level of maximum density N_{Max} is then determined by the equation:

$$\phi_G(h_S) = \frac{kT}{m} \ln \left(\frac{N_{Max}}{N_S} \right) \quad (5)$$

At this level we assume an isotropic Maxwellian distribution function.

The density above this level can be calculated from

$$n_j = 2\pi \int \int v_{\perp} f_j(v_{\perp}, v_{\parallel}) dv_{\perp} dv_{\parallel} \quad , \quad (6)$$

where f_j is the distribution function of the j th species. We require conservation of total energy K

$$\frac{m_j}{2} \left(v_{\parallel}^2 + v_{\perp}^2 \right) + m_j \phi_G + q_j \phi = K \quad , \quad (7)$$

(where ϕ is an electrostatic potential) and the 1. adiabatic invariant

$$\frac{m_j}{2} v_{\perp}^2 / B = \mu \quad . \quad (8)$$

For the stationary case the density is then given as

$$\begin{aligned} n_j &= 2\pi \iint v_{\perp} f_j(K, \mu) \frac{\partial(K, \mu)}{\partial(v_{\parallel}, v_{\perp})} dK d\mu \\ &= \sqrt{2} \pi B \iint f_j(K, \mu) \frac{1}{\sqrt{K - m_j \phi_G - q_j \phi - B\mu}} dK d\mu \quad . \quad (9) \end{aligned}$$

In Figure 1a we show ϕ_G along a magnetic field line. There are 3 important levels where the geopotentials are ϕ_G^S , ϕ_G^M , ϕ_G^O respectively. ϕ_G^M is the maximum value of the geopotential along the field lines. ϕ_G^O is the geopotential in the equatorial plane and ϕ_G^S is the geopotential at the level h_S . It is obvious that only particles with sufficient energy will be able to cross the level ϕ_G^M . Thus to calculate the density n_M the range of integration for K is from $m_j\phi_G + q_j\phi$ to infinity, and the range for μ is from 0 to $K - m_j\phi_G - q_j\phi$. And at the level M we have

$$n_{jM} = n_{jS} \exp \left\{ - \left[m_j (\phi_G^M - \phi_G^S) + q_j (\phi^M - \phi^S) \right] / kT_j \right\}, \quad (10)$$

where we have assumed $f_j(K, \mu) \propto e^{-K/kT_j}$. Requiring charge neutrality at this level determines the electrostatic potential difference $\phi^M - \phi^S$. The density N_M can then be written as

$$N_M = N_S e^{-m(\phi_G^M - \phi_G^S)/2kT}. \quad (11)$$

The distribution function at this level is still isotropic and is shown in Figure 1b.

The density at the equator was calculated by Melrose [1967] using essentially the same method. One obtains

$$\frac{N_0}{N_M} = (1 - \operatorname{erf} x_1) \exp x_1^2 - (1 - B_0/B_M)^{1/2} (1 - \operatorname{erf} x_2) \exp x_2^2$$

$$x_1^2 = \frac{m(\phi_G^M - \phi_G^O)}{2kT} \quad x_2^2 = (1 - B_0/B_M)^{-1} x_1^2 \quad (12)$$

B_M is the magnetic field strength at the level M and B_0 is the magnetic field at the equator. The density N_0 at Io's orbit ($L = 6$) is shown in Figure 2 for different temperatures T assuming an ionospheric plasma density of $5 \times 10^6 \text{ cm}^{-3}$. Beyond Io's orbit Eq. (12) predicts a decrease of $N_0/N_M \propto L^{-4}$. Clearly except for very large temperatures the magnetospheric densities predicted by Eq. (12) are too small to account for the observations.

The distribution function at the equator consists of two beams moving from one hemisphere to the other and is shown in Figure 1b. It is quite obvious that there will be a gap in the distribution function if $\phi_G^M - \phi_G^O > 0$, which will be the case along field lines with $L \geq 1.9739$ [see Michel and Sturrock 1974]. The well known Penrose criterion predicts an electrostatic instability for this distribution function independent of the value of the temperature. (Any distribution function with a gap is unstable.) This instability can, however, be quenched by the presence of some plasma particles with velocities within this gap. These particles will not have a large enough energy or magnetic moment to move back over the geopotential hill into the ionosphere. Thus any particle in the gap will be trapped in the outer magnetosphere.

Contrary to Melrose's prediction that there are no trapped particles we believe that there must be trapped particles on field lines with $L \geq 1.9739$. And, indeed, if there were no trapped particles the plasma detector onboard Pioneer 10 would have observed no plasma, because the detector is arranged in such a way that it can only measure particles with large pitch angles. Without trapped particles there would be none of these in the outer regions of the magnetosphere. Frank et al. [1975] have, however, reported considerable number densities of ions on magnetic field lines with L ranging from 2 to 10.

Michel and Sturrock [1974] suggest that Coulomb scattering of photoelectrons is sufficient to populate the outer magnetosphere and thus provide for trapped particles. But Coulomb scattering of photoelectrons is a very ineffective process unless the density of the scatterers is large. Michel and Sturrock derive a criterion for trapping of photoelectrons by Coulomb collisions; namely that the mean free path for scattering is smaller than the length of a field line between the two positions where $\phi_G = \phi_G^M$. For 10 eV photoelectrons this requires an average density $\langle n_c \rangle$ along the field line between the two geopotential maxima

$$\langle n_c \rangle \geq \frac{1.5 \times 10^5}{L^4} \text{ cm}^{-3}$$

It appears doubtful that photoelectric densities of this magnitude exist everywhere along field lines with $L < 10$.

Swartz et al. [1975] have recently determined the flux of photoelectrons escaping from the Jovian ionosphere. They find an average value for the total escape flux with energies from 3 eV to 100 eV as $10^7 \text{ cm}^{-2} \text{ s}^{-1}$. The average energy of these particles is of the order of 10 eV. Thus their average density is only about 10^{-1} cm^{-3} which is much smaller than the critical density for trapping. In other words: the photoelectrons will move from one hemisphere to the other without making a collision. The characteristic time for collisions is 10^8 s . But this does not mean that there is, on the average, 1 collision per 10^8 s and hence 1 particle trapped in 10^8 s . If this were so one could rightly argue that trapping by collision is a cumulative process and the density of trapped particles becomes large after several collision times. The point is that the photoelectrons leave the trapping region (the region between the two geopotential maxima) before they can even make one collision. The flux lost by collisions along a field lines is

$$F = F_0 (1 - e^{-x/\lambda}) \quad , \quad (13)$$

where $F_0 \sim 10^7 \text{ cm}^{-2} \text{ s}^{-1}$, x is a length along the field line and λ is the mean free path. The average total flux lost by collision is the flux of particles into the trapping region

$$F_{tr} = \frac{2}{L} \int_0^L F dx = 2 F_0 \left[1 + \frac{\lambda}{L} (e^{-L/\lambda} - 1) \right] = F_0 \frac{L}{\lambda} \quad , \quad (14)$$

for small values of L/λ . For I_0 's flux tube ($L = 6$)

$$L = 14.6 R_J = 1.2 \times 10^{11} \text{ cm} \ll \lambda \quad .$$

One may argue that although this is a very small flux it will eventually lead to a considerable density because the trapped particles are lost only by recombination which is a very slow process. If recombination is the only loss mechanism, we can estimate the average density of trapped particles. The recombination loss per unit volume is $\alpha_{RC} N^2$ where $\alpha_{RC} \approx 5 \times 10^{-12} \text{ cm}^3 \text{ s}^{-1}$ for a hydrogen plasma. The total loss due to recombination in the entire flux tube of area A is

$$\int A \alpha_{RC} N^2 dx = L \alpha_{RC} \langle N \rangle^2 \langle A \rangle \quad . \quad (15)$$

Thus we find

$$\langle N \rangle^2 = \frac{F_0}{\lambda} \frac{1}{\alpha_{RC}} \frac{A_M}{\langle A \rangle} = \frac{F_0}{\lambda} \frac{1}{\alpha_{RC}} \frac{\langle B \rangle}{E_M} \quad . \quad (16)$$

The mean free path for collisions which lead to trapping was given by Michel and Sturrock [1974] as

$$\lambda = \frac{1}{\sigma N} = \frac{\beta^4}{N \sigma_0 \cos^2 \alpha} \quad , \quad (17)$$

where α is the angle by which the particles have to be scattered in order to be trapped. This angle is the loss cone angle α which is given as

$$\sin^2 \alpha = B/B_M \quad ,$$

$\sigma_0 = 2.49 \times 10^{-25} \text{ cm}^2$ and $\beta = v/c$ is the relative velocity of the two scatterers, i.e., of 2 particles coming from the southern and northern hemisphere respectively. Taking average quantities along a field line one finds the average density is

$$\langle N \rangle = 5 \times 10^{-14} \frac{F_0}{\beta^4} \cos^2 \alpha = 2 \times 10^{-4} \frac{F_0}{E^2} \cos^2 \alpha \text{ [cm}^{-3}] \quad (18)$$

where E is measured in eV and F_0 in $\text{cm}^{-2} \text{ s}^{-1}$.

Using the values of Swartz et al. [1975] for the total flux escaping across the potential barrier, $\int_{E_M}^{\infty} j(E) dE$ where E_M is the

energy required to drag a proton across the barrier [see Ioannidis and Brice 1971], we find that the equilibrium density is 0.5 cm^{-3} at $L = 3$ and 2 cm^{-3} at $L = 10$. These are smaller than the values given by Ioannidis and Brice for two reasons. The flux of Swartz et al. is an order of magnitude smaller than the fluxes used by Ioannidis and Brice. Ioannidis and Brice also assume that all photoelectrons will be trapped by collisions whereas we have shown that only a small fraction (typically of the order of 10^{-6}) will be trapped by collisions.

It seems that Coulomb scattering cannot provide for an efficient trapping mechanism which is apparently required by the observations of Frank et al. It would only be an effective mechanism if $\lambda = 1$. We do not believe that this is the case inside $10 R_J$. Instead, we believe that the essential physics is contained in the instability created by the beams. This was already suggested by Ioannidis and Brice as well as by Goertz [1974] and Michel and Sturrock [1974]. However, no analysis of the effect of the instability on plasma densities has been published so far.

3. TRAPPING BY WAVE-PARTICLE INTERACTION

The distribution function at the equator (as shown in Figure 1b) is an inverted loss-cone distribution. It is known that this kind of distribution function is unstable [see e.g. Stringer, 1964]. Since the energy density of the beam particles is much less than the magnetic energy density we can treat the magnetic field as very large and only Landau resonances will be excited. The electric fields of the unstable waves are potential and there is no perturbation of the magnetic field. Then the wave-particle interaction will cause only one-dimensional diffusion in velocity space along the characteristics $v_{\parallel} = \text{const.}$ [Kennel and Engelmann 1966].

Numerical plasma simulations have shown that for an infinite plasma the oscillation energy attains a value of about 5-10% of the beam energy. In the case of Jupiter we do not, however, have an infinite plasma but a finite one. Furthermore, we have constant injection of beam particles into the centrifugally dominated region of the Jovian magnetosphere. Tsytovitch [1970] has shown that under these circumstances the oscillation energy can reach very high levels through a pile-up effect. The reason for this is the following: Beam particles which enter the centrifugally dominated region ($\phi_G^M - \phi_G^O > 0$) are not only acted upon by the waves they themselves generate but also by those excited earlier by other beam particles. This is so because the oscillation energy is convected along the field

lines with the group velocity $dw/dk \approx V_{th}$ which is smaller than the beam velocity. Newly arriving beam particles generate waves from an already high level created by the previous particles. This leads to a much higher level of oscillation energy. A calculation of this level of oscillation energy is beyond the scope of this paper.

Instead, we will argue that there exists a stationary level of electrostatic oscillation in the centrifugally dominated regions of the magnetosphere. Beam particles and trapped particles will interact with this random force in such a way that the loss rate due to recombination is balanced by the diffusion in velocity space.

The analysis of the interaction proceeds in the same way as in the usual derivation of the quasilinear theory. We will deal with the one-dimensional case only. Then

$$\frac{\partial f_j}{\partial t} = \frac{e^2}{m_j} \frac{\partial}{\partial v} \sum_k \int_0^\infty ds e^{-ikvs} \langle E_k(t) E_k(t-s) \rangle \frac{\partial F_j}{\partial v} \quad (19)$$

where

$$f_j = \int F_j v_\perp dv_\perp \quad (20)$$

$f_j(v_\parallel)$ is shown in Figure 3.

For stationary oscillations

$$\langle E_k(t) E_k(t-s) \rangle = \langle E_k(0) E_k(-s) \rangle \quad (21)$$

For simplicity we may assume an exponential correlation function

$$\langle E_k(t+\tau) E_k(t) \rangle = |E_k|^2 \exp(-i\omega_k \tau - a_k |\tau|) \quad (22)$$

with $a_k > 0$ and $a_k \ll \omega_k$. Then we obtain the diffusion equation

$$\frac{\partial f_j}{\partial t} = \frac{e^2}{m_j^2} \frac{\partial}{\partial v} \sum_k \frac{|E_k|^2}{i(kv - \omega_k) + a_k} \frac{\partial f_j}{\partial v} \quad (23)$$

We now replace the discrete spectrum by a continuous spectrum and consider the real part only

$$\frac{\partial f_j}{\partial t} = \frac{\partial}{\partial v} \left[\frac{2\pi e^2}{m_j^2} \int |E_k|^2 \delta(kv - \omega_k) dk \frac{\partial f}{\partial v} \right] = \frac{\partial}{\partial v} \left(\frac{D^*}{v} \frac{\partial f}{\partial v} \right)$$

$$D^* = \frac{2\pi e^2}{m_j^2} |E_k|^2 \left| \frac{\omega_k}{v} \right| \quad (24)$$

It seems plausible that the spectrum of the oscillations is flat at least within a certain range of frequencies. Here we will use $D^* = \text{const.}$ The total distribution function f_j consists of trapped particles f_j^t and beam particles f_j^b supplied by the ionosphere. First we deal with the trapped particles. For a stationary state the loss $\partial f_j^t / \partial t$ can be approximated by f_j^t / τ_{RC} which assumes a recombination coefficient independent of velocity. Then a solution of Eq. (24) which is finite at the origin is

$$f_j^t \approx C B_1' \left[v / (D^* \tau_{RC})^{1/3} \right], \quad (25)$$

where B_1 is an Ayry function. According to the arguments above, D^* is large and the argument of B_1' is small.

$$f_j^t \approx C \left[\frac{1}{\Gamma(1/3)} + \frac{1}{3^{1/2} \Gamma(2/3)} \frac{v^2}{2(D^* \tau_{RC})^{2/3}} + \dots \right] \quad (26)$$

This indicates the formation of a plateau in the velocity distribution. This is in accordance with the general conclusions of Kennel and Engelmann [1966]. The density of trapped particles is then

$$n_j^t = 2 \int_0^{w_j} f_j^t dv = 2C(D^* \tau_{RC})^{1/3} \left\{ B_1 \left[w_j / (D^* \tau_{RC})^{1/3} \right] - B_1(0) \right\} \quad (27)$$

For large values of $D^* \tau_{RC}$ this reduces to

$$n_j^t = 2Cw_j \quad . \quad (28)$$

w_j is the maximum velocity of the trapped particles

$$\begin{aligned} \frac{1}{2} (w_j^2) &= \phi_G^M - \phi_G + \frac{q_j}{m_j} (\phi^M - \phi) + \frac{2 kT_j}{m_j} \frac{B_M - B}{B} \ln \left(\frac{B_M}{B_M - B} \right) \\ &= W_{jo}^2 + \frac{2 kT_j}{m_j} \frac{B_M - B}{B} \ln \left(\frac{B_M}{B_M - B} \right) \quad . \quad (29) \end{aligned}$$

For the beam particles we assume an ionospheric source of the form

$$\frac{\partial}{\partial v} \left(\frac{D^*}{v} \frac{\partial f_j^b}{\partial v} \right) = A_j \exp \left[\left(W_{jo}^2 / v_{oj}^2 \right) \left(\frac{B_M}{B_M - B} \right) \right] e^{-v^2 / v_{oj}^2} \left(\frac{B_M}{B_M - B} \right) \quad (30)$$

for $|v_{||}| > W_{jo}$ and

$$\frac{\partial}{\partial v} \left(\frac{D^*}{v} \frac{\partial f_j^b}{\partial v} \right) = 0 \quad ,$$

for $|v_{||}| < W_{jo}$

$$v_{oj}^2 = 2 kT_j^2 / M_j \quad .$$

The life time τ of the beam particles can be calculated as the ratio of the total beam density to the diffusion loss

$$\tau = \frac{\int f_j^b dv}{\int \frac{\partial}{\partial v} \frac{D^*}{v} \left(\frac{\partial f_j^b}{\partial v} \right) dv} = \frac{v_{oj}^4}{2 D^* w_j} \left(\frac{B_M - B}{B_M} \right)^2 \quad . \quad (31)$$

The mean free path of a beam particle is of the order of τw_j or the characteristic wavelength of the oscillations times the ratio of thermal energy to oscillation energy. As a rough estimate we take the wavelength as the beam velocity divided by the beam plasma frequency or $10^{-4} v_b^{3/2} / F^{1/2}$. For $F = 10^6 \text{ cm}^{-2} \text{ s}^{-1}$ and $v_b = 10^8 \text{ cm}$ this becomes 10^5 cm and the mean free path is smaller than the length of a field line even if the energy of the oscillations is only 1/100 of the thermal energy. Under these conditions nearly all the beam particles will be trapped. Then we can calculate the density n_j^t by equating the loss due to recombination to the total flux provided by the ionosphere and not to only $F_o(\lambda/s)$ as in the case of Coulomb's collisions.

$$F_{MM}^A \approx 4 \int_0^{s_M} \alpha_{RC} (Cw_j)^2 A(s) ds \quad (32)$$

where $s = 0$ in the equatorial plane. We anticipate that the trapped particle density is much larger than the beam density. Then charge neutrality requires that $W_e^2 = W_i^2$ combining Eqs. (29) and (32) we finally obtain for the trapped particle density

$$N^t = \left[\frac{F_M}{\alpha_{RC} I(L)} \right]^{1/2}, \quad (33)$$

where

$$I(L) = R_M \int_0^{s_M} \frac{W_i^2}{B(s)} ds \quad (34)$$

For the temperature of the beam particles we take the characteristic energy of the escaping photoelectrons. For $F_M = 10^6 \text{ cm}^{-2} \text{ s}^{-1}$, $\alpha_{RC} = 5 \times 10^{-12}$ and a surface field of 4 Gauss the trapped particle density in the equatorial plane is shown in Figure 4. For $L < 4$ the density must level off because the basic assumption that all the flux will be trapped is not valid anymore. This effect is difficult to calculate because it requires a knowledge of the diffusion constant D^* and hence the spectrum of the electrostatic wave noise. Inside $L = 2$ no trapping occurs and the density will fall to values predicted by Eq. (12) which are very small. The solid curve in Figure 4 represents the values obtained by Eq. (33), whereas the dotted curve is an indication of the effect of reducing the flux. The dashed line in

Figure 4 represents the density limit obtained by Gledhill [1967] and Michel and Sturrock [1974] for a surface field of 4 G. At $L \approx 30$ the plasma density will reach this critical value and one would expect serious distortions of the magnetic field beyond that distance. It is interesting to note that Goertz et al. [1974] find that the magnetic field observed by Pioneer 10 can be represented by the dipole field plus a perturbation field due to a current sheet which starts at $30 R_J$. However, even at distances smaller than $30 R_J$ the drift motion of the plasma particle should provide for a current density and hence a distortion of the field. Then our method of calculating N^t , which depends on the assumption of a dipole field, is not valid anymore. Thus the densities outside say $15 R_J$ can not be considered as very realistic.

4. COMPARISON WITH OBSERVATIONS

Figure 5 shows equidensity contour plots inside $15 R_J$ calculated from $N_j^t = Cw_j$. The insert compares the values from the model with those inferred by Frank et al. from their observations. The agreement is quite good considering the assumptions made in the model and the uncertainties of the observations. Figure 5 displays clearly the disk-like shape of the plasma distribution first suggested by Gledhill [1967] which, however, he derived from somewhat different assumptions. The relatively dense plasma will cause a stretching of the field lines beyond $15 R_J$ which has the effect of making the disk thickness smaller because of the dependence of Cw_j on $B(s)$ and radial distance.

It should be obvious from the previous section that velocity space diffusion due to Landau resonances will leave the perpendicular energy of the particles unaffected. Thus we expect the trapped particle distribution to have a perpendicular temperature comparable to the ionospheric temperature. The parallel "temperature" should be much larger. Frank et al. have measured protons with characteristic energies of 100 eV. At present it is impossible to tell from their data whether the particle distributions are isotropic or not. Assuming a Maxwellian distribution for the perpendicular velocities, we predict an anisotropic directional flux of the form

$$j(E, \alpha) = AE e^{-E \sin^2 \alpha / kT} (1 + bE \cos^2 \alpha) \quad (35)$$

which, however, is a strongly varying function of pitch angle α only for small values of α . It is doubtful that an effective temperature of 100 eV could be explained by this dependence on α , particularly as the minimum value of α at which Frank et al. measured proton fluxes is about 40° . Thus their characteristic energies are representative of the perpendicular energy and little can be said about the parallel energy. It should be noted that the spin modulation of the fluxes mentioned by Frank et al. may be related to the anisotropy described by Eq. (36). It seems, however, difficult to separate this effect from the spin modulation due to penetrating high energy particles. We find it more likely that the relatively large energies reported by Frank et al. are indicative of a genuine heating of the proton's perpendicular energy. There are two possibilities which one might invoke to explain the large observed perpendicular energies.

Trapped particles remain in the outer regions for a long time and are eventually lost only by recombination. The time scale for recombinations is $\tau_{RC} \sim 2(\alpha \frac{n}{N^+ e^-})^{-1}$. For $\alpha \frac{n}{N^+ e^-} \sim 5 \times 10^{-12} \text{ cm}^3 \text{ s}^{-1}$ this is of the order of 10^{10} s at $L = 6$. The time scale for Coulomb collisions is only several hours. Clearly the trapped particles will undergo many collisions before they are lost by recombination. These collisions will eventually lead to an isotropic distribution with a thermal energy of about $1/3$ of the parallel energy $\frac{1}{3} w_j w_j^2$. Figure 6

shows $\frac{1}{2} m_i w_i^2$ in the equatorial plane as a function of distance from the planet. We assume again that T_e is of the order of the energy of the escaping photoelectrons. These energies are generally of the right order of magnitude. But they are representative of the parallel energy. For an isotropic distribution the energies would be smaller than the observed ones by at least a factor of 6. The energy of the trapped electrons $\frac{1}{2} m_e w_e^2$ is smaller than this by a factor of m_e/m_i if charge neutrality is valid.

A second possibility of increasing the perpendicular energy may be a mechanism which was suggested by Kern [1962] for the earth's magnetosphere. He shows that repeated hydromagnetic shock waves accelerate particles trapped in the magnetosphere. For perpendicular shocks only the perpendicular energy is changed. He considers the shock waves as being generated by a sudden compression of the front side of the magnetosphere by increases in the solar wind pressure. At some distance in the magnetosphere the solar wind compresses the magnetosphere faster than the local hydromagnetic wave velocity and the compression pulse propagates as a shock wave. If the rise time of the shock is smaller than an ion gyroperiod ions will not conserve their adiabatic moment, but the magnetic moment of a trapped particle is increased as it is swept up by the shock. The subsequent slow relaxation of the compression conserves the adiabatic moment and after the magnetic field returns to its initial value the perpendicular energy ($E_{\perp} = \mu B$) will be larger than before the shock event. The energy

gain of an ion by a single shock is not large enough to explain Frank's result. But if particles are subject to a number of shocks it is conceivable that their perpendicular energies increase considerably. Kern finds that proton energies of up to several keV can be obtained by this process in the earth's magnetosphere.

If the time between successive shocks is large compared with the time for collisions we would not expect this process to be important. We do, however, know by now that the Jovian magnetosphere is extremely variable in size and that the solar wind does indeed push the magnetosphere in. Several events have been witnessed by both Pioneer 10 and 11 [see e.g. Smith et al. 1975, Wolfe et al. 1974]. Kern finds that the transverse kinetic energy density ϵ_n in the undisturbed medium after n shock events is increased above the transverse energy density ϵ_0 in the undisturbed medium by

$$\epsilon_n = \epsilon_0 2^{-2n} \left[\left(\frac{U_0}{C_1} \right)^{1/3} + \left(\frac{C_1}{U_0} \right)^{1/3} \right]^{2n} \quad (36)$$

where U_0 is the velocity of the compression pulse and C_1 is a local Alfvén velocity. For a shock we must have $U_0 > C_1$. Since this process leaves the density unchanged we would expect the perpendicular energy to increase as

$$E_{\perp} = E_{\perp 0} 2^{-2n} \left[\left(\frac{U_0}{C_1} \right)^{1/3} + \left(\frac{C_1}{U_0} \right)^{1/3} \right]^{2n}$$

beyond the distance where $U_0 > C_1$. Since the Alfvén velocity ($C_1 = B/\sqrt{4\pi m_1 N}$) decreases with distance this process may conceivably lead to an increasing perpendicular energy. However, a typical Alfvén velocity inside $r = 10 R_J$ is 2×10^8 cm/s, and one would require very fast compressions for this mechanism to work. There is little hope that this mechanism can account for the 100 eV protons observed inside Io's orbit. It may be active in the distant parts of the magnetosphere and in part responsible for the energetic protons required for the observed perturbation of the magnetic field.

Since there is very little doubt that Frank's energies refer to perpendicular energies the above arguments show that there must be a mechanism active in the Jovian magnetosphere which heats the ions. If, as Frank et al. assume, the observed ions come from the Jovian ionosphere and have indeed a temperature of 100 eV everywhere along the field lines, there must be a very large density of extremely hot ions in the ionosphere. Then the geopotential barrier is relatively unimportant, the plasma is collision dominated everywhere and the treatment above is irrelevant. But then one encounters the usual difficulties of a model in which the plasma is in statistical equilibrium (see section 2). On the other hand, the assumption of an outside source (say the solar wind) and radial diffusion would not be able to explain the fact that the energy decreases with decreasing distance unless severe energy losses were involved. Furthermore, the solar wind could not supply the large densities observed. We believe

that the energization of the ions must take place along field lines. The following is a very speculative attempt to describe such a mechanism.

In the previous section we have assumed charge neutrality everywhere along a field line. This may not be a valid assumption. It has been speculated that particle acceleration along field lines in the earth auroral ionosphere is due to potential double layers [see e.g. Block 1972 and references therein]. Potential double layers are small regions where charge neutrality is not valid and strong electric fields exist.

These double layers, or electrostatic shocks, presumably form when a mechanism exists through which an appropriate distribution function for trapped particles (i.e., those which are reflected by the double layer) can be maintained. Recent computer simulations [Goertz and Joyce 1975] have shown that stable double layers can be generated under certain circumstances. Knorr and Goertz [1974] have described double layers in the framework of BGK solutions of the Vlasov equation. They find that strong double layers require distribution functions for trapped particles which have a minimum at $v = 0$, precisely those one would obtain in the Jovian magnetosphere. The potential drop across a double layer may well obtain many kT/e as in the numerical simulations. Two double layers, one in the northern hemisphere and one in the southern hemisphere, would accelerate the ions and at the same time prevent them from escaping along field lines into the

opposite hemisphere. Figure 7 is a sketch of the possible location of these structures. Although this model may explain the large observed energies much more work is needed in order to assess the possibilities of the various mechanisms mentioned. However, this seems impossible without any further information about the pitch angle distribution of the trapped protons.

5. DISCUSSION

In the previous sections we have shown that the Jovian ionosphere can provide enough plasma to explain the observations of Frank et al. We also showed that an ion-heating mechanism seems to be required. Note that as long as a strong diffusion is valid the trapped particle density is independent of the characteristic temperature of the trapped particles. In this section we want to discuss two consequences of our model, one relating to the densities only and the other relating to the large characteristic energies of the trapped particles.

It is known [Kennel and Petschek 1966] that the stably trapped high energy particle fluxes are determined by the intensity of whistler mode noise. Particles above a certain critical energy, which scales like $B^2/8\pi N$, are pitch angle scattered and lost more rapidly to the ionosphere than particles with smaller energies. Figure 8 shows how $B^2/8\pi N$ varies with distance (assuming a dipole field of 4 G surface strength). These values are not unlike the values at which Baker and Van Allen [1975] and Filius et al. [1974] observe a change in the energy spectrum of the electrons. A detailed analysis of the energy spectra is being undertaken at present and the results will be published elsewhere.

Because the characteristic energy of the trapped particles is rather large, certain ideas about the distribution of plasma in the magnetosphere may not be valid. In particular, Gledhill [1967], Goertz [1972] and Hill et al. [1974] have predicted that the thermal plasma should be confined to a centrifugal symmetry surface which is inclined with respect to the magnetic equatorial plane but which is not parallel to the rotational equatorial plane either. This is due to the fact that the centrifugal force tends to push the plasma to the most distant point (from the rotational axis) along a field line. This argument is, however, only valid if the centrifugal force is much larger than the magnetic force, i.e.,

$$\frac{1}{2} \Omega^2 r^2 \cos^2 \lambda \gg \frac{1}{B} \left(\frac{1}{2} v_{\perp}^2 + v_{\parallel}^2 \right) \nabla B$$

This inequality is true for a low-temperature plasma. But in the Jovian magnetosphere the energy of the plasma is at least comparable, if not larger, than the corotational energy $m\Omega^2 r^2/2$. Thus, the inequality is not fulfilled in the Jovian magnetosphere. Indeed, it seems much more likely that the inequality is actually reversed. Then the particles are confined to the magnetic equatorial plane. Without a knowledge of the pitch angle distribution of the trapped particles we cannot decide whether the inequality is reversed or not. There is some experimental evidence, derived from Pioneer 10 magnetic field data [Goertz et al. 1974], which indicates that the thermal

plasma is confined to the magnetic equatorial plane. Clearly, more information on the plasma distribution and temperatures is needed in order to decide these questions and assess the validity of the model presented. It is our sincere hope that a proper plasma experiment will be included on future Jupiter probes.

REFERENCES

- Anderson, J. D., G. W. Null and S. K. Wong, Gravity Results from Pioneer 10 Doppler Data, 79, 3661 (1974).
- Baker, D. N. and J. A. Van Allen, Energetic Electrons in the Jovian Magnetosphere, Univ. of Iowa Research Report 75-13 (1975).
- Block, L. P., Potential Double Layers in the Ionosphere, Cosmic Electrodyn., 3, 349 (1972).
- Filius, R. W. and C. E. McIlwain, Measurements of the Jovian Radiation Belts, J. Geophys. Res., 79, 3589 (1974).
- Frank, L. A., K. L. Ackerson, J. H. Wolfe and J. D. Mihalov, Observations of Plasmas in the Jovian Magnetosphere, Univ. of Iowa Research Report 75-5 (1975).
- Gledhill, J. A., Jupiter's Magnetosphere, Nature, Lond., 214, 156 (1967).
- Goertz, C. K., Ph.D. Thesis, Rhodes University, Grahamstown, South Africa (1972).
- Goertz, C. K., Jupiter's Ionosphere and Magnetosphere, Planet. Space Sci., 13, 95 (1974).
- Goertz, C. K. and G. Joyce, Numerical Simulation of the Plasma Double Layer, Astrophys. and Space Sci., 32, 165 (1975).
- Goertz, C. K., R. A. Randall and M. F. Thomsen, A Model for the Jovian Magnetosphere, EOS, 56, 1172 (SM50) (1974).

- Hill, T. W., A. J. Dessler and F. C. Michel, Configuration of the Jovian Magnetosphere, Geophys. Res. Letters, 1, 3 (1974).
- Ioannidis, G. and N. Brice, Plasma Densities in the Jovian Magnetosphere: Plasma Slingshot or Maxwell Demon?, Icarus, 14, 380 (1971).
- Kennel, C. F. and F. Engelmann, Velocity Space Diffusion from W Plasma Turbulence in a Magnetic Field, Phys. of Fluids, 9, 2377 (1966).
- Kennel, C. F. and H. E. Petschek, Limit on Stably Trapped Particle Fluxes, J. of Geophys. Res., 71, 1 (1966).
- Kern, J. W., A Note on the Generation of the Main-Phase Ring Current of a Geomagnetic Storm, J. of Geophys. Res., 67, 3737 (1962).
- Knorr, G. and C. K. Goertz, Existence and Stability of Strong Potential Double Layers, Astrophys. and Space Sci., 31, 209 (1974).
- Melrose, D. B., Rotational Effects on the Distribution of Thermal Plasma in the Magnetosphere of Jupiter, Planet. Space Sci., 15, 381 (1967).
- Michel, F. C. and P. A. Sturrock, Centrifugal Instability of the Jovian Magnetosphere and its Interaction with the Solar Wind, Planet. Space Sci., 22, 1501 (1974).
- Piddington, J. H., Jupiter's Magnetosphere, Univ. of Iowa Preprint 67-63.
- Smith, E. J., L. Davis, Jr., D. E. Jones, P. J. Coleman, Jr., D. S. Colburn, P. Dyal, C. P. Sonett and A. M. A. Frandsen, The Planetary Magnetic Field and Magnetosphere of Jupiter: Pioneer 10, J. Geophys. Res., 79, 3501 (1974).

Smith, E. J., L. Davis, Jr., D. E. Jones, P. J. Coleman, Jr., P.

Dyal, C. P. Sonett and A. M. A. Frandsen, Jupiter's Magnetic Field, Magnetosphere and Interaction with the Solar Wind, to be published in Science (1975).

Stringer, T. E., Electrostatic Instabilities in Current-Carrying

and Counter-Streaming Plasmas, J. Nucl. Energy. 16, 267 (1964).

Swartz, E. W. R. W. Reed and T. R. McDonough: Photoelectron Escape

from the Ionosphere of Jupiter, J. of Geophys. Res., 80, 495 (1975).

Wolfe, J. H., J. D. Mihalov, H. R. Collard, D. D. McKibbin, L. A. Frank

and D. S. Intriligator, Pioneer 10 Observations of the Solar Wind Interaction with Jupiter, J. Geophys. Res., 79, 3489 (1974).

FIGURE CAPTIONS

- Figure 1a The variation of the geopotential along a field line. The curve is not drawn to scale.
- Figure 1b The distribution functions of particles from the ionosphere at the levels S, M and O.
- Figure 2 Collisionless densities in the equatorial plane at $6 R_J$ for different ionospheric temperatures.
- Figure 3 The parallel distribution function $f_j = \int F_j v_{\perp} dv_{\perp}$.
- Figure 4 Equatorial trapped particle densities. For a description of this figure refer to the text.
- Figure 5 Equidensity contour plots. The contours are in intervals of 10 cm^{-3} . This figure does not take into account the tilt of the dipole with respect to the rotational axis.
- Figure 6 Characteristic energies of trapped particles. The dots indicate some "temperatures" observed by Frank et al. [1975].
- Figure 7 A sketch of the possible location and polarity of potential double layers in the Jovian magnetosphere.
- Figure 8 The magnetic energy per particle ($B^2/8\pi N$) in the equatorial plane as a function of distance from Jupiter.

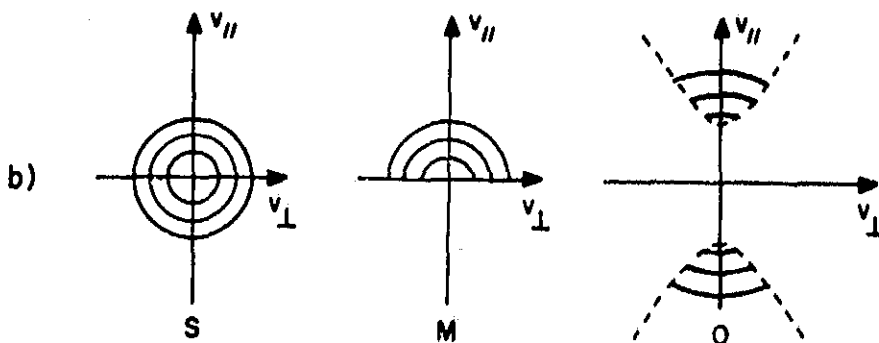
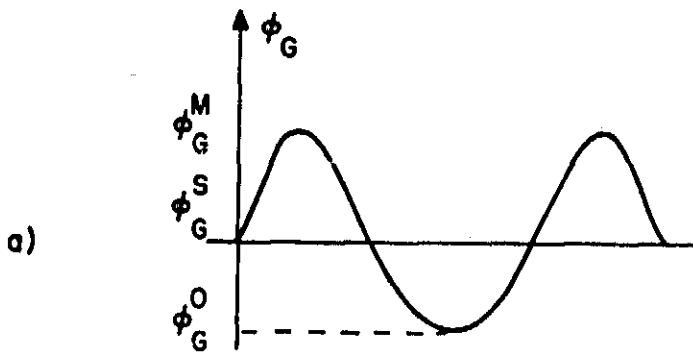
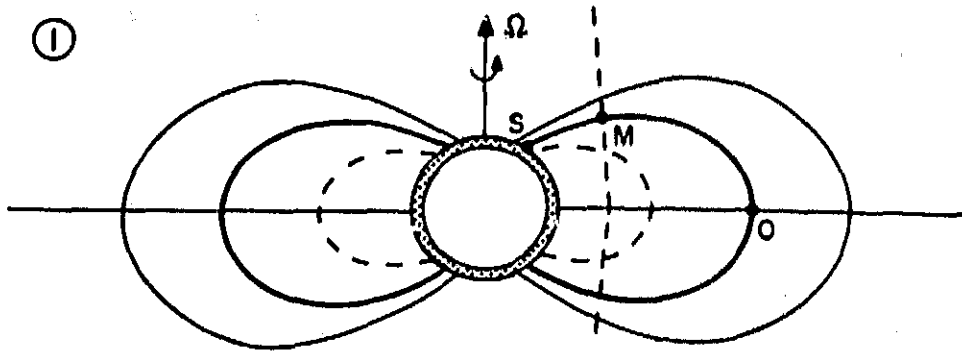


FIGURE 1a and 1b

A-675-214

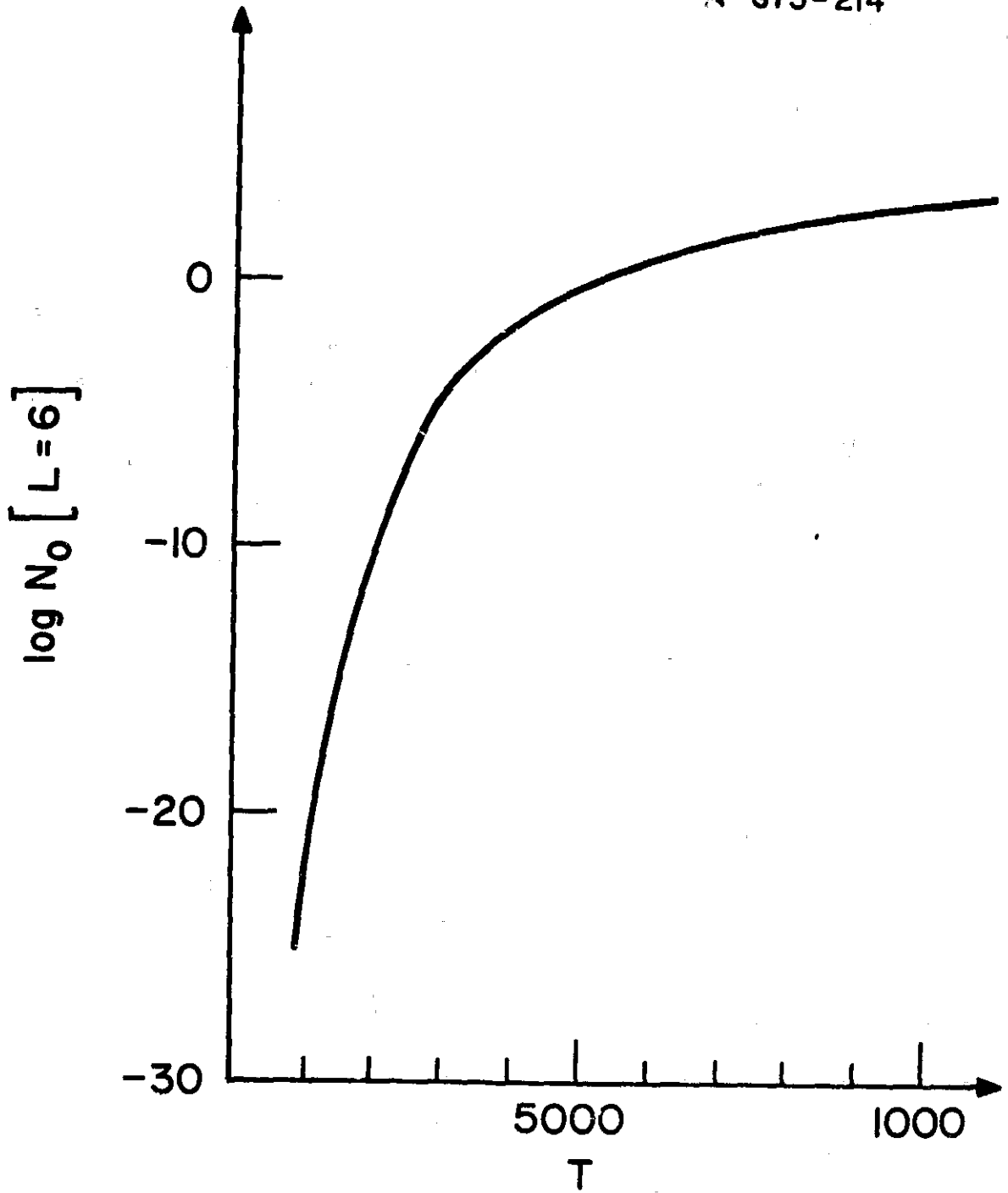


FIGURE 2

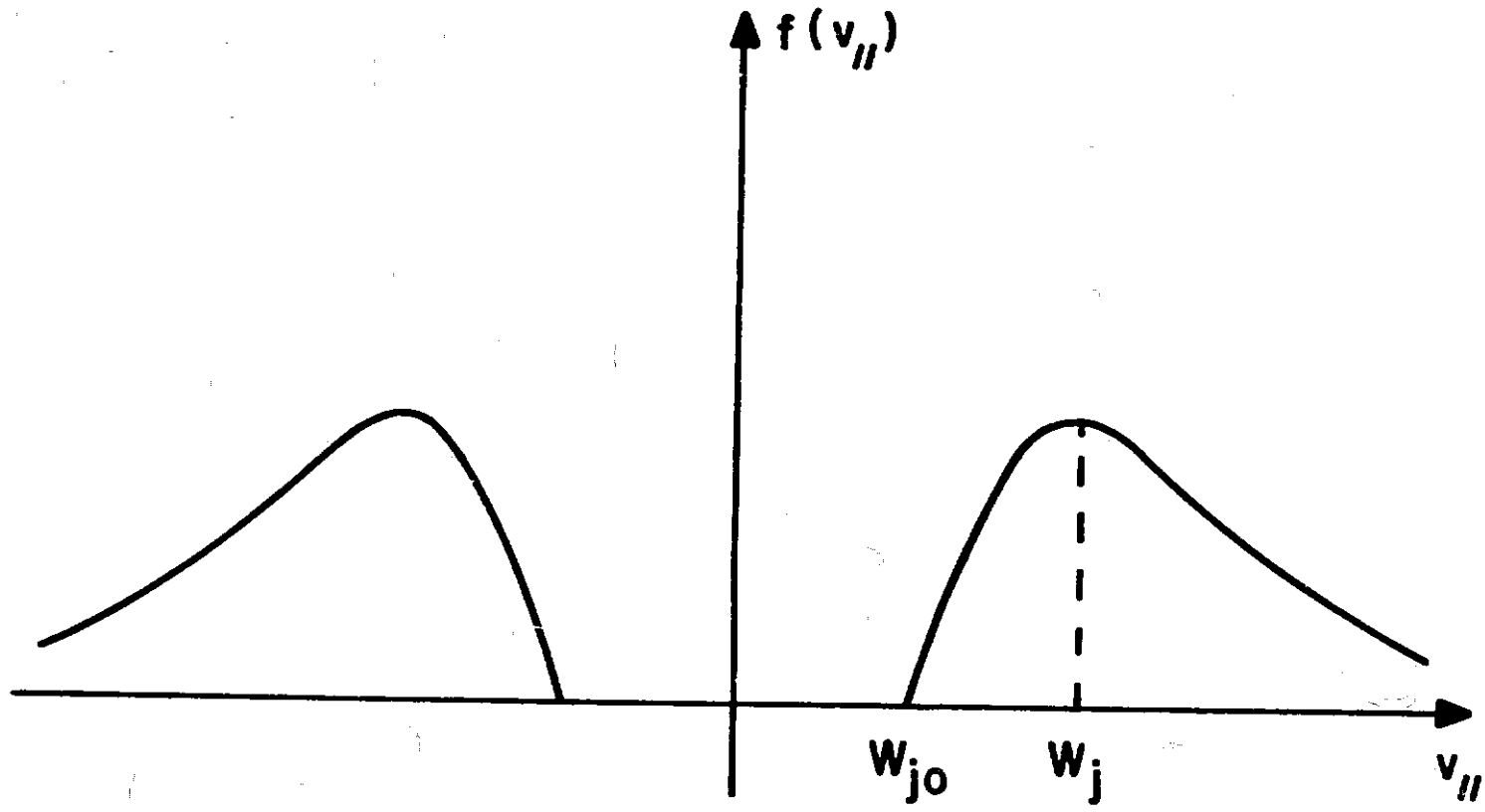


FIGURE 3

A-G75-217

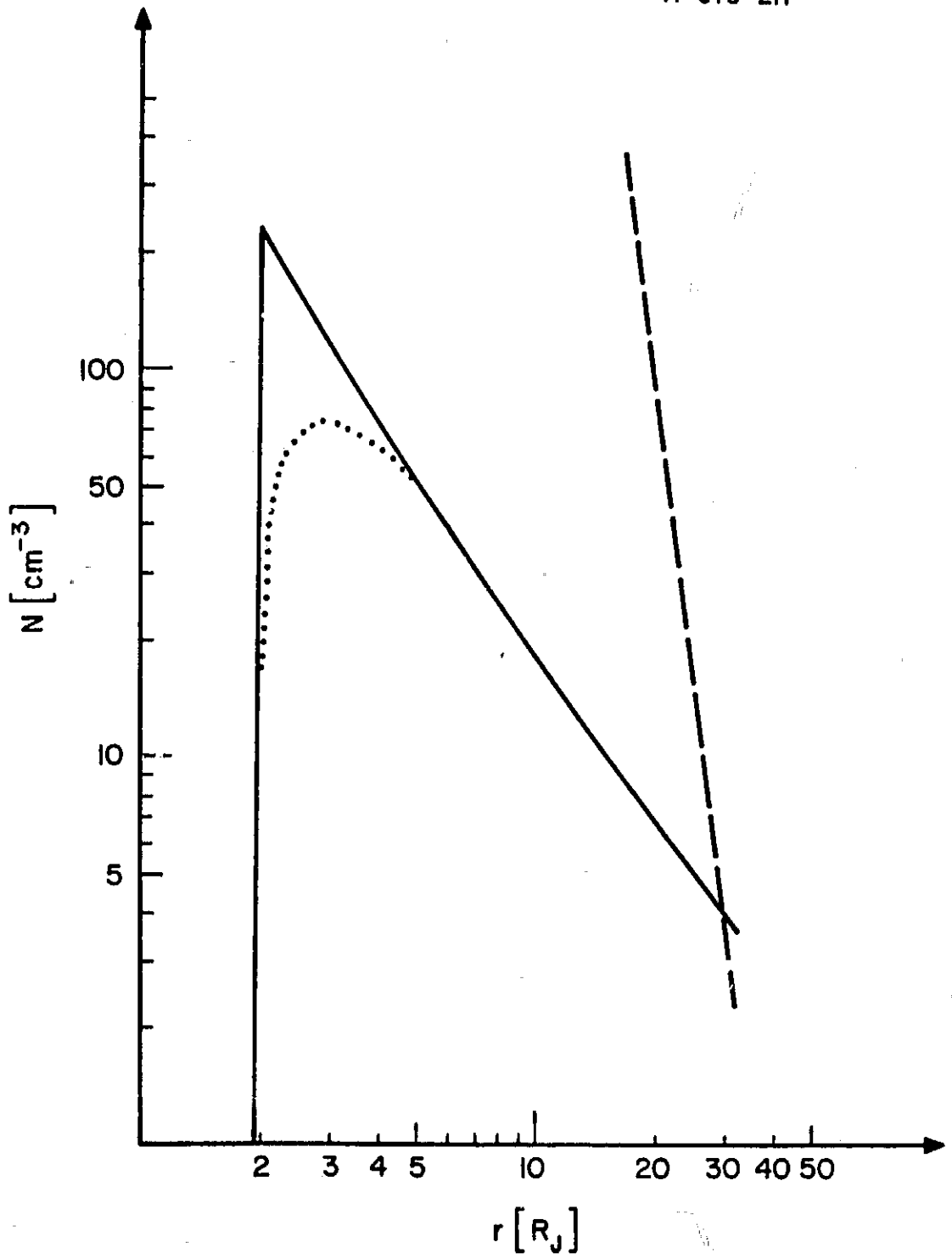


FIGURE 4

A-675-216

| | N_{obs} | N_{model} |
|---|-----------|-------------|
| 1 | 80 | 70 |
| 2 | 30 | 30 |
| 3 | 30 | 20 |
| 4 | 15 | 20 |

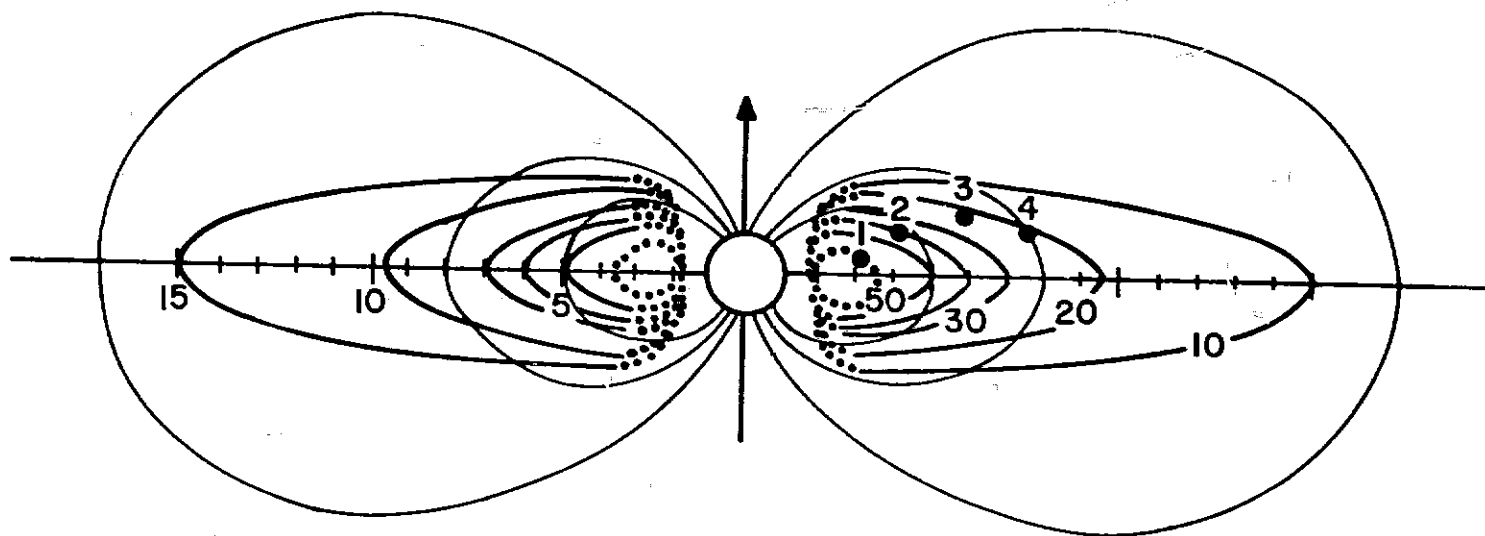


FIGURE 5

44

A-G75-213

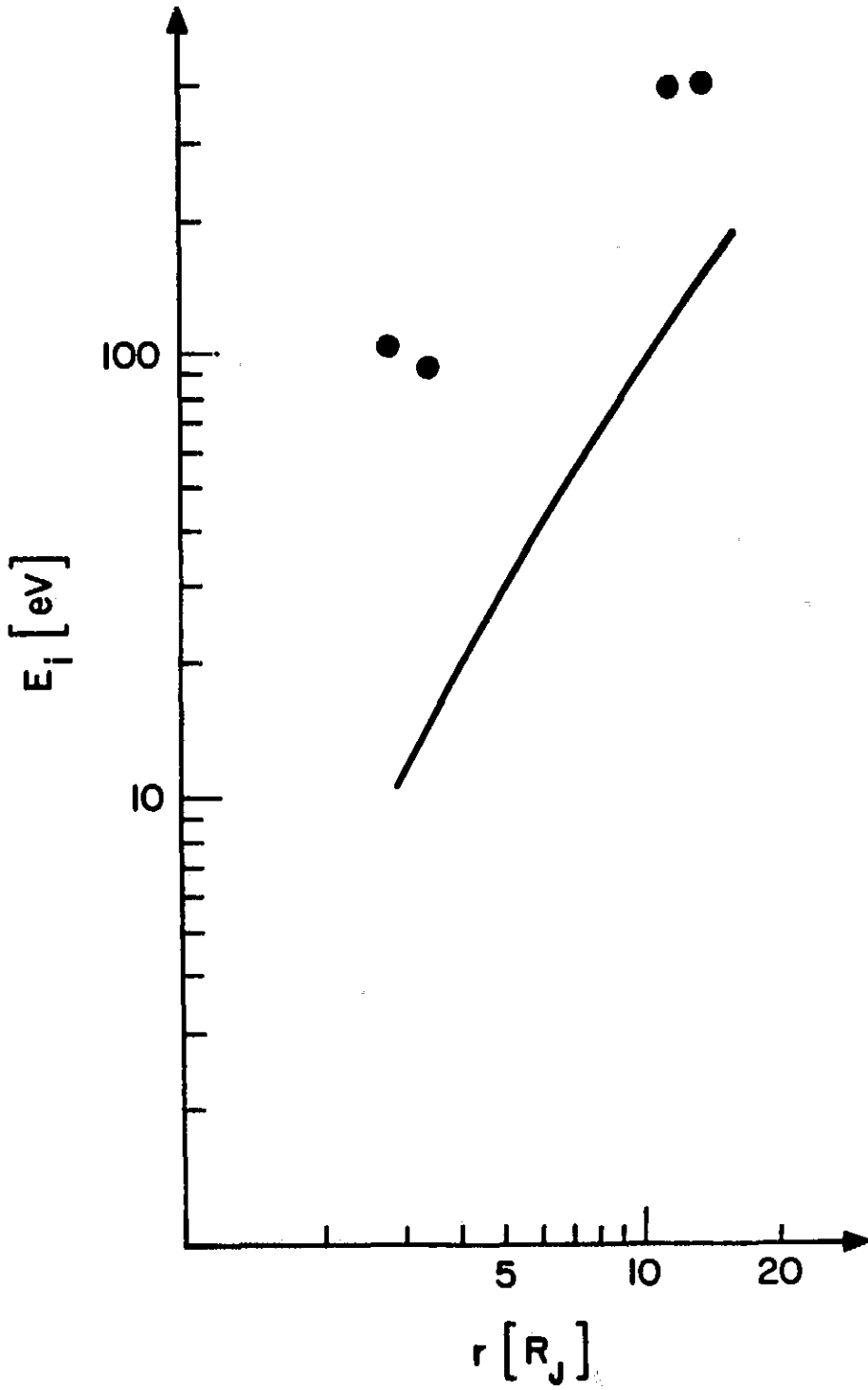


FIGURE 6

A-675-215

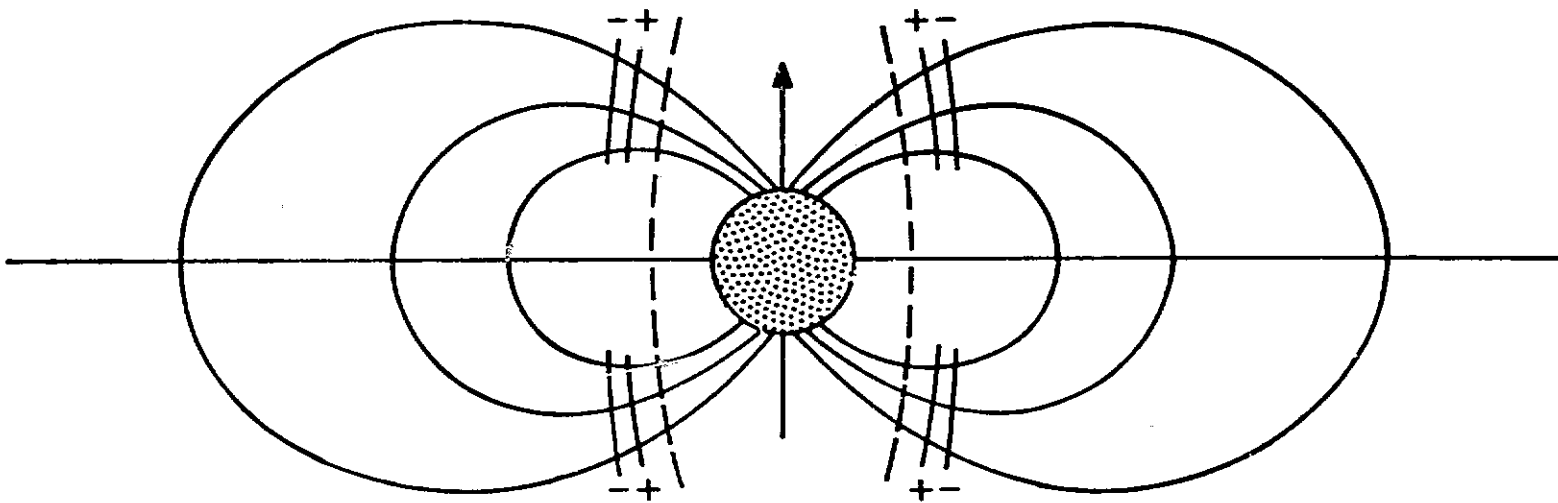


FIGURE 7

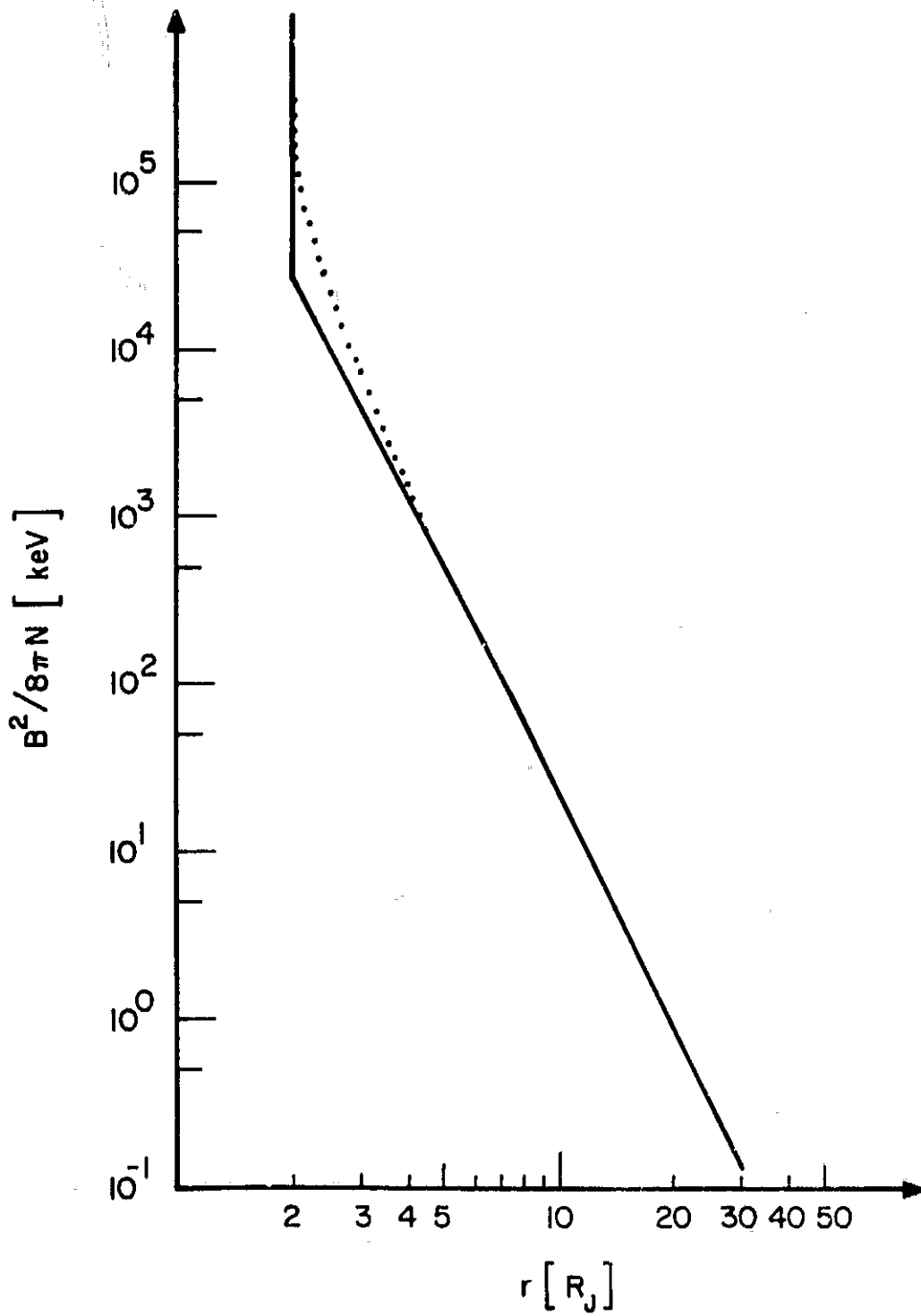


FIGURE 8